A Balloon Shape Monopole Super Wideband MIMO Antenna for THz Applications

Sachin Agrawal, Prabhat Kumar Soni

Abstract – **A balloon shape super wideband (SWB) Terahertz monopole antenna and its pattern diversity configuration are presented in this paper. In order to enhance the impedance bandwidth, the feedline is tapered. It improves impedance matching and results in large impedance bandwidth. Both antenna element and diversity configuration offers an almost equal impedance bandwidth of about 186% for |S11| ≤ -10dB. In the case of the antenna element, the lower edge of frequency response is at 2.11 THz whereas, in the diversity case it is 2.17 THz. However, the upper edge of the frequency point is the same (60 THz) in both cases. Besides, isolation of more than 25 dB throughout the band is achieved between antenna elements. The overall antenna element and MIMO configuration size are 24×41.8 μm2 and 70.8×42 μm2, respectively. The parameters like Diversity Gain (DG), Envelop Correlation Coefficient (ECC), Channel Capacity Loss (CCL) and Mean Effective Gain (MEG) are calculated to characterize the diversity performance and all are found in the acceptable limit.**

Keywords – **Super wideband applications, MIMO applications, Pattern diversity applications, Monopole antenna, Impedance bandwidth**

I. INTRODUCTION

The developing era of wireless technology creates a huge demand for wideband antennas which can support a high data rate transmission and provide improved efficiency. The Terahertz (THz) frequency band starting from 0.1-10 THz or higher is mainly assigned for this purpose [1-5]. In this context, various wideband planar [6-14] and non-planar antennas like Yagi Uda [15], helix [16], helical [17], horn [18], leaky-wave, lens [19] have been proposed in the recent past. However, the planner structure is found to be the most suitable because of its small size and ease of integration with compact devices. Nowadays one of the major problems with wideband THz antenna is the loss of signal due to fading in a multipath environment. The multiple input multiple output (MIMO) seems to be a promising technology. It mitigates the possibility of signal fading and tends to increase the channel capacity and spectral efficiency as well. On the other side, isolation arises due to the accommodation of multiple elements in MIMO configuration. Therefore, current trends in MIMO antenna are towards bandwidth and isolation enhancement. In literature, various planar MIMO super wideband (SWB) antennas have been proposed for THz applications [20-26].

Sachin Agrawal and Prabhat Kr. Soni are with the Department of Electronics and Communication Engineering, National Institute of Technology, Delhi India, E-mail: sachinagrawal@nitdelhi.ac.in, 212220007@nitdelhi.ac.in

However, most of them tender either high bandwidth with a large antenna size or narrow bandwidth with a compact antenna. For an instant, a tetradecagonal ring-shaped MIMO antenna for THz application is reported in [21].

For pattern diversity configuration, it offers a huge bandwidth of about 194%, but at the cost of a large antenna footprint of $800×600×81.29$ μm^3. Similarly, an elliptical shape super wideband (SWB) MIMO antenna with high isolation is presented in [22]. Although, the designed structure supported adequate impedance bandwidth of 184% but with a huge antenna size of $1000×1400×101.29$ μm^3. A fractal MIMO antenna is proposed in [26]. It obtained an impedance bandwidth of 173% from 0.72 THz to 10 THz with a compact size however, the fractal geometry increases the complexity of the design.

In this paper firstly, a compact balloon-shaped monopole super wideband antenna for THz application is designed and analysed. To accomplish the wide bandwidth, both the feedline and radiator are tapered. It has been demonstrated that after tapering the feedline and radiator the impedance matching is significantly improved and results in huge impedance bandwidth of 186% from 2.1 THz to 60 THz or more. In the next section, a MIMO antenna is designed by placing two identical antennas orthogonally. It endows more than 25dB isolation throughout the frequency range. In addition, the diversity performance measuring parameters like diversity gain (DG), envelope correlation coefficient (ECC), mean effective gain (MEG) and channel capacity loss (CCL) are calculated. It is found that in the entire frequency range, the ECC is less than 0.0008, diversity gain is almost constant at 10, and MEG is less than -3dB.

II. ANTENNA DESIGN AND RESULTS DISCUSSION

Figure 1 illustrates the geometry of the proposed SWB antenna. It is designed on FB-4 substrate of the dielectric constant of 2.65 and thickness of 1μm. As seen, the top layer of the substrate consists of a balloon shape radiator excited by the tapered feedline. Whereas, the bottom layer of the substrate comprises a rectangular ground plane of length 19.8 μm. Further, the feedline and the vertices of the radiator are tapered, in order to enhance the bandwidth of the proposed antenna. The antenna's optimized dimensions are listed in Table I.

The antenna design steps and the corresponding scattering parameters are illustrated in Fig. 2 and Fig. 3, respectively. The results show that the antenna has very poor impedance matching when it comprises a rectangular patch fed by a microstrip feedline. A small improvement is observed after

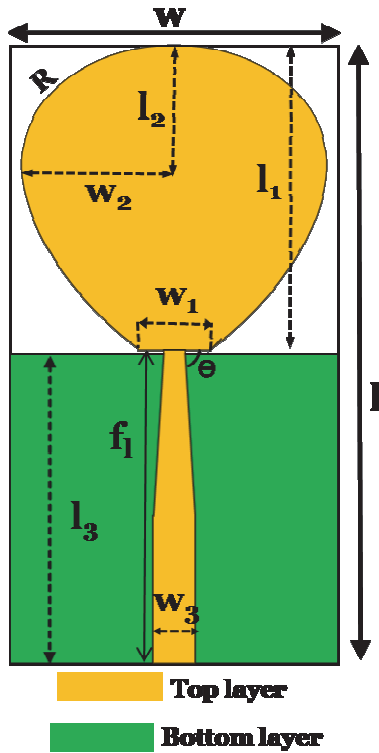tapering the feedline by the angle of $\ominus$= 5° as shown in step-2 of Fig. 2.

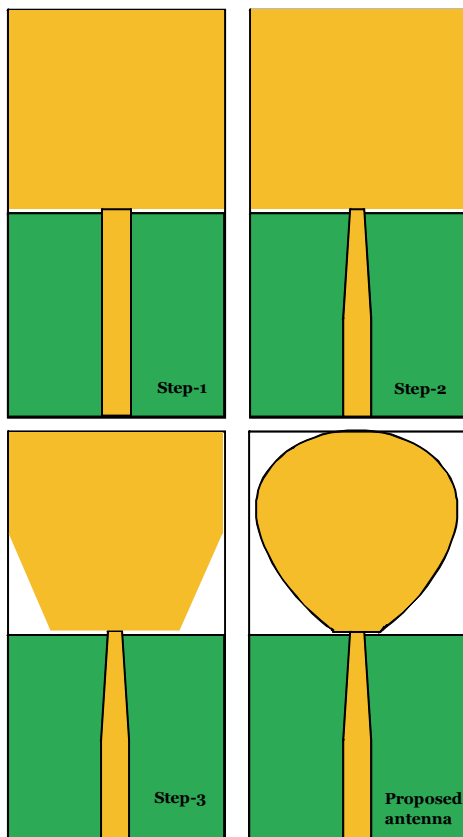Fig. 1. Geometry of the proposed antenna

Fig. 2. Design evaluation of the proposed SWB THz antenna

TABLE I
OPTIMIZED DIMENSIONS OF THE PROPOSED SWB THZ ANTENNA

Dimensions	Value (µm)	Dimensions	Value (µm)	Dimensions	Value (µm)
w	24	w_2	9.7	d	7.3
l	41.8	l_1	21.5	w_d	73.8
l_2	9.6	w_1	4	h_d	8.9
l_3	19.8	w3	3	l_d	41.8

In the third step, the lower vertices of the patch are tapered, wich tremendously improves the matching throughout the frequency range and results in a large impedance bandwidth. Here, it can be noticed that the lower frequency edge of frequency response remains unaffected by the tapering of the patch and feedline. Finally, in the fourth step, the patch is further blended at all its vertices to get an additional improvement as depicted in Fig. 3. As seen, the proposed antenna design achieved an impedance bandwidth of more than 186% from 2.1 THz to 60 THz or more.
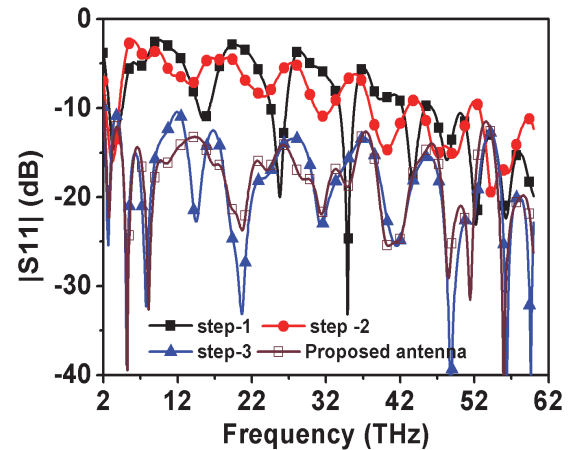

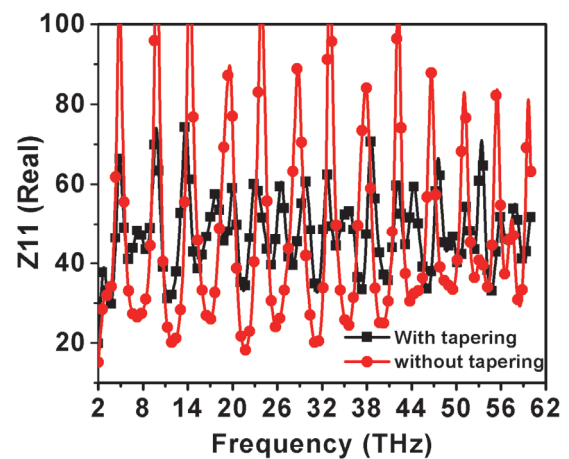Fig. 3. Simulated |S11| corresponds to different design steps

Fig. 4. Input impedance variation with and without feedline tapering

Figure 4 illustrates the input impedance variation with and without feedline tapering. It can be noticed that the antenna input impedance becomes closer to 50 Ω after tapering of the feedline with a tapering width of 10 μm. The gain comparison of step 3 and step-4 of the proposed SWB antenna is displayed in Fig. 5. As seen, tapering all corners of the radiator as shown in step-4 of Fig. 2 tends to increase the gain throughout the frequency range. It can be seen that the peak gain of the proposed antenna is 8.3 dBi. The radiation efficiency is depicted in Fig.6. It can be observed that the antenna tenders above 90% efficiency throughout the band.
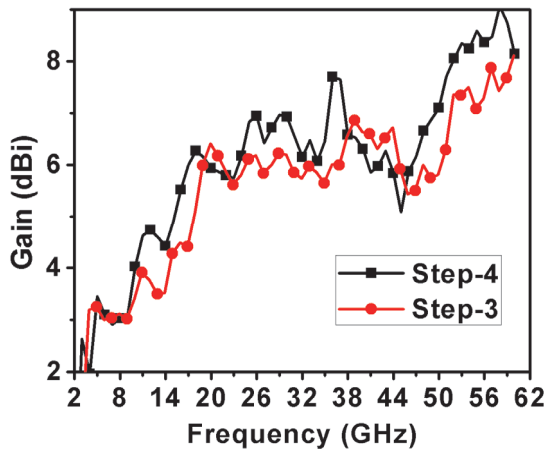
down the same antenna structure for different frequency bands with almost the same bandwidth (i.e. 186%). Here, λ_l is the wavelength corresponding to the lower cutoff frequency of the antenna.

To validate the above design equations two test antennas have been simulated for lower (1-40 THz) and upper (4-60 THz) frequency bands. Figure 7 illustrates the simulated |S11| of antennas under test. It can be noticed that both antennas properly cover the said frequency band and follows the same pattern.
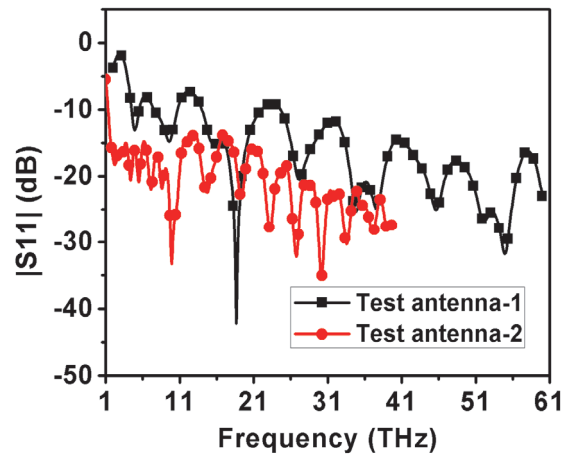
Fig. 5. Gain comparison of the proposed SWB THz antenna

Fig. 7. |S11| of antennas under test

Fig. 6. Efficiency of the proposed SWB THz antenna
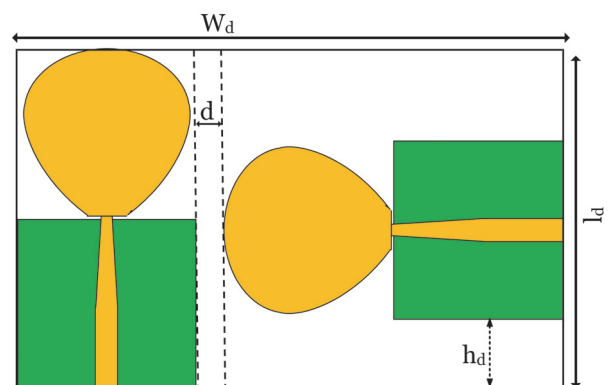
Fig. 9. Scattering parameters of the proposed diversity configuration

TABLE II
ANTENNA DESIGN PARAMETERS TO SCALE UP AND SCALE DOWN THE DESIGN

Parameters	W	l	f_l
Value	$0.176\lambda_l$	$0.306\ \lambda_l$	$0.148\ \lambda_l$
Parameters	L3	R	
Value	$0.145\ \lambda_l$	$0.198\ \lambda_l$	

In order to scale the proposed antenna in other frequency bands some design equations have been prepared and shown in Table II. Using these parameter values one can scale up and
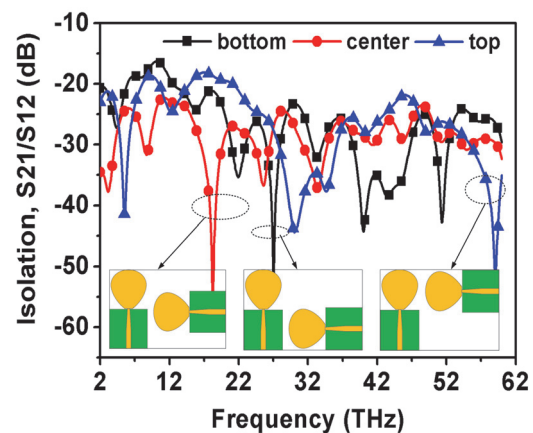
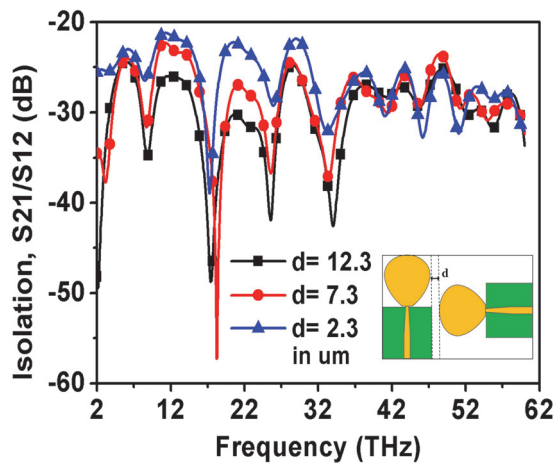Fig. 10. Isolation, S21/S12 for different orientation of antenna-2

Fig. 11. Isolation, S21/S12 for different distance between antenna-1 and antenna-2
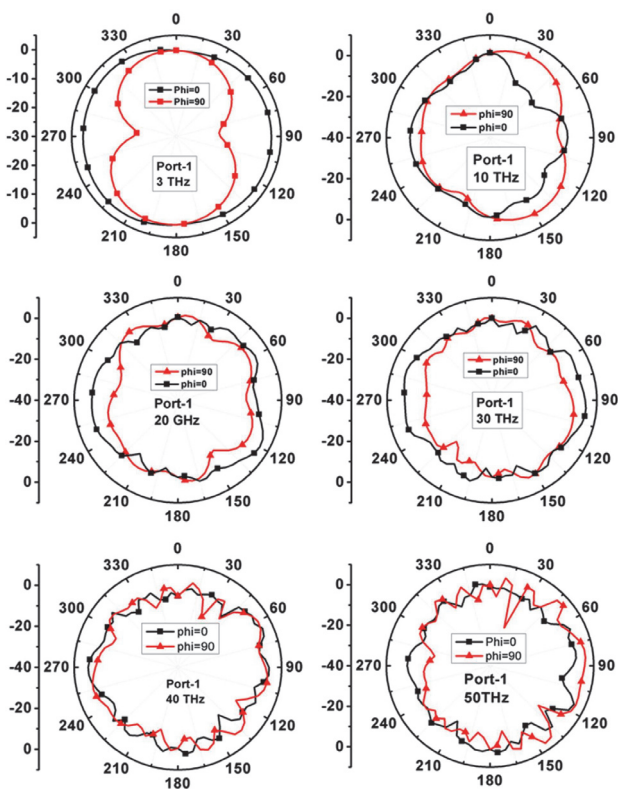

Fig. 12. Radiation patterns at six different frequencies for port 1 of pattern diversity configuration

Further, the pattern diversity configuration is realized by orthogonally placing two copies of the proposed antenna as depicted in Fig. 8. The scattering parameters of the MIMO configuration are illustrated in Fig. 9. It can be seen that |S11| and |S22| are identical to each other. For both ports, the lower edge frequency point is at 2.17 THz and the upper one is more than 60 THz. The isolation (S21/S12) between the ports is more than 25 dB throughout the frequency range. Here, initially the orthogonally placed antenna-2 is kept at the centre position, which is varied up and down to find the optimum value of the isolation. Fig. 10 shows the isolation (S21) for different values of the height of antenna-2 from the ground plane. As seen the maximum isolation is achieved for the

centrally located orthogonal antenna as compared to the other two combinations. Figure 11 demonstrates the isolation (S21) for different values of distance (d) between both antenna elements by keeping other antenna parameters constant. Here, it is worth mentioning that antenna-2 is centrally placed. It can be seen that between 6 THz to 32 THz, the isolation level is improved gradually by increasing the distance between both antennas. However, it increases the footprint of the MIMO configuration. In this work, the distance (d) is kept at 7.3 μm to make the MIMO compact.
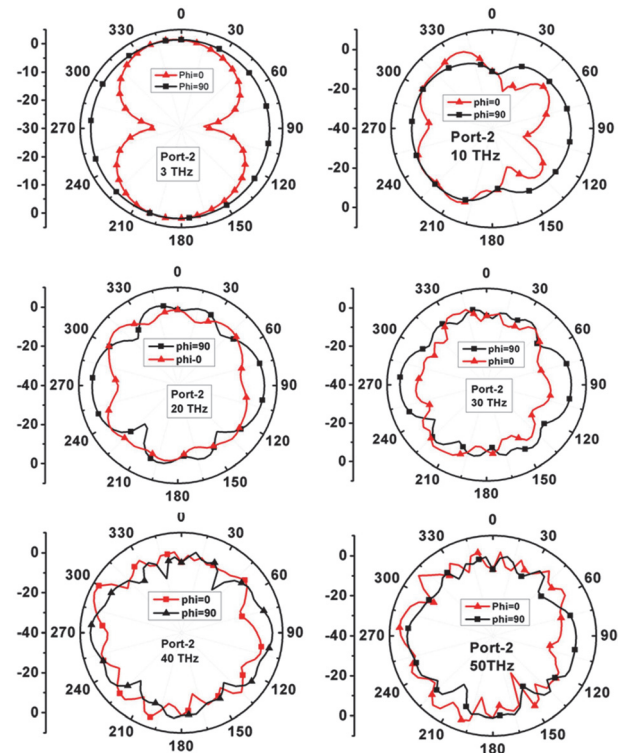

Fig. 13. Radiation patterns at six different frequencies for port 2 of pattern diversity configuration

The radiation patterns for port-1 and 2 are depicted in Fig. 12 and Fig. 13, respectively. As observed for each frequency point, the radiation patterns at Phi= 0° of port-1 are the same as the radiation patterns at Phi=90° of port-2. This inter changeability of the radiation pattern between port-1 and port-2 indicates that the proposed MIMO antenna achieved pattern diversity. To further justify the diversity performance of the proposed antenna some more parameters like Envelop Correlation Coefficient (ECC), Diversity Gain (DG) and Channel Capacity Loss (CCL) are investigated. For an uncorrelated MIMO system, the ideal value of ECC should be zero, however, for a satisfactory operation, its value should be ≤ 0.5. Figure 14(a) displays the ECC (calculated from the S-parameters) of the proposed MIMO antenna. It can be observed that the proposed design accomplished an acceptable ECC level which is less than 0.0002 in the maximum portion of the frequency range. Figure 14(b) shows the diversity gain of the MIMO antenna. It exhibits an admissible diversity gain (ideally ≈10), varying between 9.99 to 10. The channel capacity loss (CCL), which signifies the maximum limit of lossless message transfer rate in a communication channel is illustrated in Fig. 15(a).

TABLE III
PERFORMANCE COMPARISON OF THE PROPOSED SWB THZ ANTENNA WITH RECENTLY PUBLISHED WORK

Ref.	Frequency range &	Wavelength (corresponds to lower freq.) λ_l (μm)	bandwidth (THz)	Bandwidth (%)	Antenna size (μm3)	Conducting material
[5]	0.46-5.46	651.7	5	168.92	800×600×81.29	Copper
[6]	0.46-8.84	651.7	8.38	187.8	600×600×81.29	Copper
[7]	0.53-8	565.6	7.47	175.1	600×600×81.29	Copper
[8]	0.1-10	2997.9	9.9	196	150×150×20	Copper
[9]	0.58-6.6	516.8	6.02	167.6	400×600×81.29	Copper
[11]	0.434-1.684	690.7	1.25	118.04	150×150×9.6	Copper
[12]	128 GHz	-	128 GHz	20.65	500×500×50	Copper
[13]	26.7 GHz	-	26.7 GHz	3.9	208×180×10	Copper
[14]	0.61-.065	491.4	34.92 GHz	5.56	800×600×191.29	Copper
[20]	3.1-more than 60 THz	96.7	>56.9 THz	>179.8	110×65×10	Copper
[21]	0.3-15.1	999.3	14.8 THz	192.2	800×600×81.29	Copper
[23]	2.6-60	115.3	57.4 THz	>183.3	24×41.8×1	Copper
[25]	0.86-100	348.5	99.14 THz		110×74×16	Copper
Proposed	2.11-more than 60 THz	142.7	>57.84 THz	>186	24×41.8×1	Copper

As seen, CCL is in the lossless message transfer and below the permissible limit (i.e.< 0.4 bits/S/Hz) in the entire frequency range. Further, the mean effective gain (MEG), defined as a ratio of the received power by the diversity antenna and the received power by an isotropic antenna is depicted in Fig. 15 (b). It reveals that the MEG-1 and MEG-2 are equal and close to -3 dB. These results indicate that the proposed SWB MIMO antenna design attains diverse performance. The performance comparison of the proposed SWB antenna with the recently reported THz antennas is demonstrated in Table III. As seen, the designed antenna offered a reasonable impedance bandwidth with a smaller antenna size.

III.   CONCLUSION

This paper presents an SWB MIMO antenna for THz applications. It offers a wide impedance bandwidth of around 186% from 2.11 THz to more than 60 THz. To scale up and down the antenna structure for different frequency bands two design guidelines have also been prepared and validated by simulation of two test antennas. Further, a 2×2 MIMO antenna has also been proposed with an isolation of more than -25 dB throughout the frequency range. In addition, various diversity performance measurement parameters like CCL, MEG, DG and ECC are calculated and all are found in the permissible limits. The result shows that the proposed MIMO

antenna tenders ECC less than 0.0002 in most of the frequency regions and 0.0008 through the band.

REFERENCES

[1]   S. Koenig, D. Lopez-Diaz, J. Antes, F. Boes, R. Henneberger, A. Leuther, A. Tessmann, R. Schmogrow, D. Hillerkuss, R. Palmer, T. Zwick, C. Koos, W. Freude,O. Ambacher, J. Leuthold and I. Kallfass, "Wireless Sub-THz Communication System with High Data Rate", *Nature photonics*, vol .7, no. 12, pp. 977- 981, 2013.

[2]   D. Woolard, R. Brown, M. Pepper, M. Kemp, "Terahertz Frequency Sensing and Imaging: A Time of Reckoning Future Applications", *Proc. IEEE*, vol. 93, no. 10, pp. 1722–1743, 2005.

[3]   S. Galoda and G. Singh, "Fighting Terrorism with Terahertz", *Ieee Potentials*, vol. 26, no. 6, pp. 24–29, 2007.

[4]   V. Krozer, T. Löffler, J. Dall, A. Kusk, F. Eichhorn, R. K. Olsson, J. D. Buron, P. U. Jepsen, V. Zhurbenko and T. Jensen, "Terahertz Imaging Systems with Aperture Synthesis Techniques", *IEEE Transactions on Microwave Theory and Techniques*, vol. 58 no. 7, pp. 2027–2039, 2010.

[5]   S. Singhal, "Ultrawideband Elliptical Microstrip Antenna for Terahertz Applications", *Microwave and Optical Technology Letters*, vol. 61, no. 10, pp. 2366-2373, 2019.

[6]   U. Keshwala, S. Rawat and K. Ray, "Inverted K-Shaped Antenna with Partial Ground for THz Applications", *Optik*, vol. 219, p.165092, 2020.

[7] V. Das and S. Rawat, "Modified Rectangular Planar Antenna with Stubs and Defected Ground Structure for THz Applications", *Optik*, vol. 242, p.167292, 2021.

[8] S. Das, D. Mitra and S.R.B. Chaudhuri, "Fractal Loaded Circular Patch Antenna for Super Wide Band Operation in THz Frequency Region", *Optik*, vol. 226, p.165528, 2021.

[9] U. Keshwala, S. Rawat and K. Ray, "Design and Analysis of Eight Petal Flower Shaped Fractal Antenna for THz Applications", *Optik*, vol. 241, p.166942, 2021.

[10] K. R. Jha and G. Singh, "Analysis and Design of Terahertz Microstrip Antenna on Photonic Bandgap Material", *Journal of Computational Electronics*, vol. 11, no. 4, pp.364-373, 2012.

[11] H. Davoudabadifarahani and B. Ghalamkari, "High Efficiency Miniaturized Microstrip Patch Antenna for Wideband Terahertz Communications Applications", *Optik*, vol. 194, p.163118, 2019.

[12] M. N. E. Temmar, A. Hocini, D. Khedrouche, et al., "Analysis and Design of a Terahertz Microstrip Antenna Based on a Synthesized Photonic Bandgap Substrate Using BPSO", *Journal of Computational Electronics*, vol. 18, no. 1, pp. 231–240, 2019.

[13] S. Ullah, C. Ruan, T. U. Haq and X. Zhang, "High Performance THz Patch Antenna Using Photonic Band Gap and Defected Ground Structure", *Journal of Electromagnetic Waves and Applications*, vol. 33, no. 15, pp.1943-1954, 2019.

[14] R. K. Kushwaha, P. Karuppanan and L.D. Malviya, "Design and Analysis of Novel Microstrip Patch Antenna on Photonic Crystal in THz", *Physica B: Condensed Matter*, vol. 545, pp.107-112, 2018.

[15] K. Han, T. K. Nguyen, I. Park and H. Han, "Terahertz Yagi-Uda Antenna for High Input Resistance", *Journal of Infrared, Millimeter, and Terahertz Waves*, vol. 31, no. 4, pp.441-454, 2010.

[16] L. Guo, F. Huang and X. Tang, "A Novel Integrated MEMS Helix Antenna for Terahertz Applications", *Optik*, vol .125(1), pp.101-103, 2014.

[17] Z. R. Hajiyat, A. Ismail, A. Sali and M. N. Hamidon, "Design and Analysis of Helical Antenna for Short-Range Ultra-High-Speed THz Wireless Applications", *Optik*, vol. 243, p.167232, 2021.

[18] A. Gonzalez, K. Kaneko, T. Kojima, S. Asayama, Y. Uzawa, "Terahertz Corrugated Horns (1.25-1.57 THz): Design, Gaussian Modeling, and Measurements", *IEEE Trans. Terahz. Sci. Technol.* vol. 7, no. 1, pp. 42–52, 2017.

[19] X. Wang, W. Zhao, J. Hu, W. Yin, "Reconfigurable Terahertz Leaky Wave Antenna Using Graphene-Based High-Impedance Surface", *IEEE Trans. Nanotechnol.* vol.14, no. 1, pp. 62–69, 2015.

[20] S. Singhal, "Four Arm Windmill Shaped Superwideband Terahertz MIMO Fractal Antenna", *Optik*, vol. 219, p.165093, 2020.

[21] Singhal, S., "Tetradecagonal ring shaped terahertz superwideband MIMO antenna". Optik, vol. 208, p.164066, 2020.

[22] G. Saxena, Y. K. Awasthi and P. Jain, "High Isolation and High Gain Super-Wideband (0.33-10 THz) MIMO Antenna for THz Applications", *Optik*, vol. 223, p.165335, 2020.

[23] S. Singhal, "Asymmetrically Fed Trapezoidal Superwideband Pattern Diversity Antenna", *Optik*, vol. 231, p.166358, 2021.

[24] G. Varshney, S. Gotra, V. S. Pandey and R. S. Yaduvanshi, "Proximity-Coupled Two-Port Multi-Input-Multi-Output Graphene Antenna with Pattern Diversity for THz Applications", *Nano Commun. Net.*, vol. 21, p.100246, 2019.

[25] S. Singhal, "CPW Fed Circular Sierpinski Terahertz Antenna for Superwideband Pattern Diversity Applications", *Optik*, p.167430, 2021.

[26] S. Das, D. Mitra and S. R. B. Chaudhuri, "Fractal Loaded Planar Super Wide Band Four Element MIMO Antenna for THz Applications", *Nano Commun. Net.*, vol. 30, p.100374, 2021.
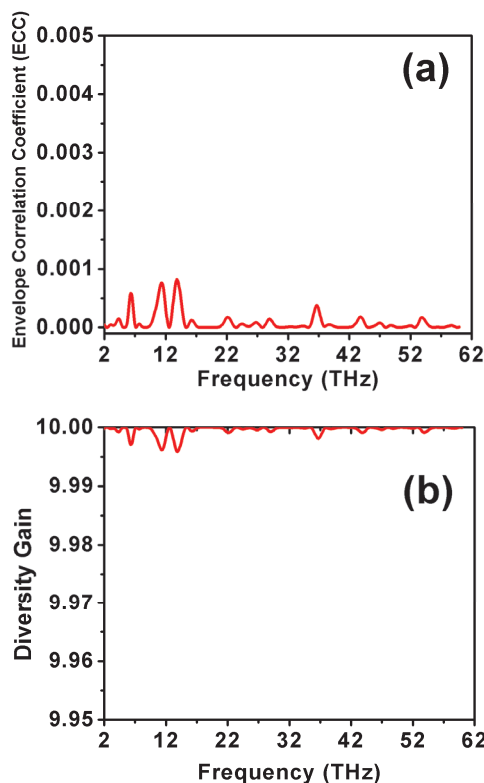

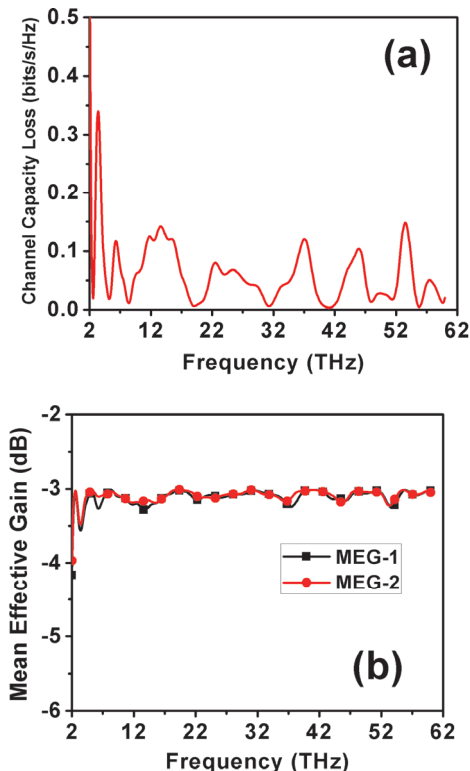Fig. 14. (a) Envelope correlation coefficient (ECC), (b) Diversity gain (DG) of the proposed antenna

Fig. 15. (a) Channel capacity loss, (b) Mean effective gain